

## Monte Carlo studies of extensions of the Blume-Emery-Griffiths model

C. C. Loois, G. T. Barkema and C. M. Morais Smith  
 Institute for Theoretical Physics, Utrecht University,  
 Leuvenlaan 4, 3584 CE Utrecht, The Netherlands  
 (dated: February 20, 2024)

We extend the Blume-Emery-Griffiths (BEG) model to a two-component BEG model in order to study 2D systems with two order parameters, such as magnetic superconductors or two-component Bose-Einstein condensates. The model is investigated using Monte Carlo simulations, and the temperature-concentration phase diagram is determined in the presence and absence of an external magnetic field. This model exhibits a rich phase diagram, including a second-order transition to a phase where superconductivity and magnetism coexist. Results are compared with experiments on Cerium-based heavy-fermion superconductors. To study cold atom mixtures, we also simulate the BEG and two-component BEG models with a trapping potential. In the BEG model with a trap, there is no longer a first order transition to a true phase-separated regime, but a crossover to a kind of phase-separated region. The relation with imbalanced fermion mixtures is discussed. We present the phase diagram of the two-component BEG model with a trap, which can describe boson-boson mixtures of cold atoms. Although there are no experimental results yet for the latter, we hope that our predictions could help to stimulate future experiments in this direction.

## I. INTRODUCTION

Mixtures of  $^3\text{He}$  and  $^4\text{He}$  atoms exhibit a rich phase diagram, where besides a normal phase, there is a phase where  $^4\text{He}$  is superfluid, and a phase separated region of superfluid  $^4\text{He}$  and normal  $^3\text{He}$ .<sup>1</sup> In 1971, Blume, Emery and Griffiths<sup>2</sup> proposed a model to describe such mixtures. They simplified the continuous phase of the superfluid order parameter such that it could acquire only two values. Although they made this very rough approximation and modelled the uniform system in a lattice, their results are very interesting. Qualitatively, they reproduced the right phases and the right orders of the phase transitions. Furthermore, if disorder is introduced by placing the mixture into aerogel, after some modifications,<sup>3</sup> the model can still yield the experimentally observed phase diagram.<sup>4</sup>

Here, we generalize this model to a two-component case in order to describe systems with two order parameters and study the problem numerically, using Monte Carlo simulations. The motivation for the model we are proposing is twofold. Firstly, we would like to study condensed matter materials like heavy fermions, high- $T_c$  superconductors, and organic superconductors. In particular, we want to study the interplay between magnetic and superconducting ordering in these materials. Both order parameters are modelled as an Ising spin variable. Concerning the magnetism, we consider the ferro- and the antiferromagnetic cases, and investigate also the effect of an external magnetic field. We find that in the absence of a magnetic field, in the region where the two orders coexist, the system is always phase separated. When we add a magnetic field, we also find regions with microscopic coexistence of the two phases. Secondly, we want to study mixtures of cold atoms. Cold atoms have emerged in recent years as an ideal simulator of condensed matter systems. Because experiments with cold atoms are often carried out in a trap, we add a trapping

potential to the model. This fact qualitatively changes the physics of the problem. For the case of a single component BEG model in a trap, the results are compared with experimental and theoretical work on imbalanced Fermion mixtures. For the case of the two-component BEG model, we make predictions for the phase diagram of boson-boson mixtures.

The outline of this paper is the following: in section II, we introduce the two-component BEG model, and investigate it in the presence and absence of an external magnetic field. The effect of a trapping potential is described in section III. In section IV, we compare the results with magnetic superconductors and cold atom systems. Our conclusions are presented in section V.

## II. THE TWO-COMPONENT BLUME-EMERY-GRIFFITHS MODEL

The BEG model was originally proposed to describe superfluidity.<sup>2</sup> The phase diagram found by Monte Carlo simulations exhibits large similarities with the phase diagram of  $^3\text{He}$ - $^4\text{He}$  mixtures measured by experimentalists.<sup>1</sup> The main idea of studying superfluidity with the BEG model relies on the  $U(1)$  symmetry-breaking of the ground-state wave function. For superconductivity and Bose-Einstein condensation we have the same symmetry breaking, hence we can try to model these phenomena in the same way.

Several physical systems exhibit two unequal symmetry broken phases simultaneously. A general Hamiltonian describing this class of systems reads

$$H = \sum_{\langle ij \rangle} J_1 X_{ij} + \sum_{\langle ij \rangle} J_2 S_i S_j + D \sum_i X_i^2 + H \sum_i X_i \quad (1)$$

where  $(X_i; S_i)$  can take the values  $(0; 1)$ ;  $(0; -1)$ ;  $(1; 0)$ , and  $(-1; 0)$ . This choice implies that only one kind of bo-

son can occupy each lattice site.  $D$  is an anisotropy field that controls the number of lattice sites with nonzero  $s_i$ .  $H$  plays the role of an external magnetic field, which may couple only to the order parameter describing a magnetic transition. The Hamiltonian (1) is appropriate for describing phase transitions which require two order parameters, one describing the ordering of the fraction of the system with nonzero  $s$ , the other one of nonzero  $s$ . This yields several possibilities, both fractions can model superfluidity, superconductivity, or (anti)ferromagnetism. Possible applications could be magnetic superconductors, or two-component Bose-Einstein condensates.

From now on, we will consider the fraction with non-negative  $s$  as describing magnetism, and  $s$  superconductivity (preformed bosons that can Bose-Einstein condensate). Thus,  $s_i$  represents the spin of particle  $i$  and  $s_i$  the discretized phase of the wavefunction. Therefore,  $J_1$  can be both positive (ferromagnetism) and negative (antiferromagnetism), but  $J_2$  has to be positive. We define the concentration, the ferromagnetic, antiferromagnetic, and superconducting order parameters as

$$c = \frac{1}{N} \sum_i s_i^2; \quad (2)$$

$$m_{fm} = \frac{1}{N} \sum_i s_i; \quad (3)$$

$$m_{af} = \frac{1}{N} \sum_i (-1)^i s_i; \quad (4)$$

$$m_s = \frac{1}{N} \sum_i s_i; \quad (5)$$

Note that  $m_{fm}$  and  $m_{af}$  can reach a maximum value of  $c$ , and  $m_s$  of 1. We define the ratio between the two coupling constants  $J_2$  and  $J_1$  as

$$K = \frac{J_2}{J_1}; \quad (6)$$

#### A. The M method

We investigate this model by Monte Carlo simulations. To determine the location of second-order phase transitions, we performed simulations at constant concentration, in which the elementary moves were flips of  $s$  and  $s$  or nonlocal spin exchanges. The location of the transition is then obtained from the peak location of the magnetic susceptibility. The locations of first-order phase transitions are obtained from simulations at constant temperature, with as elementary moves local flips of  $s$  and  $s$ , as well as same-site replacements of  $s_i$  by  $s_i$  and vice versa. A jump in the concentration  $c$  as a function of the anisotropy field  $D$  is then the signature of the phase transition.

All simulations are performed on lattices with approximately  $40 \times 40$  sites. Per point in the phase diagram, simulations were run over  $3 \times 10^6$  to  $3 \times 10^7$  Monte Carlo steps per site, depending on the correlation times.

#### B. Zero magnetic field, $H = 0$

In the absence of a magnetic field, the Hamiltonian (1) has ferro-antiferromagnetic symmetry.

First, we consider  $K = 1$ . In this case,  $J_1 = J_2$ , and the shape of the phase diagram must be symmetric under the transformation  $c \rightarrow 1 - c$ . The results of the simulations are plotted in Fig. 1. We see that it indeed obeys this symmetry and exhibits four phases: a superconducting phase (S), where the order parameter  $m_s$  is nonzero, a ferromagnetic phase (FM), where  $m_{fm}$  is nonzero, a phase-separated regime (PS) where the spins and the angular phases have formed ordered clusters, and finally the normal phase (N), in which there is neither order nor phase separation. Analogous to the BEG model, the transition from the phase-separated regions to other phases are first-order (dashed line), the other ones are second-order (continuous line).

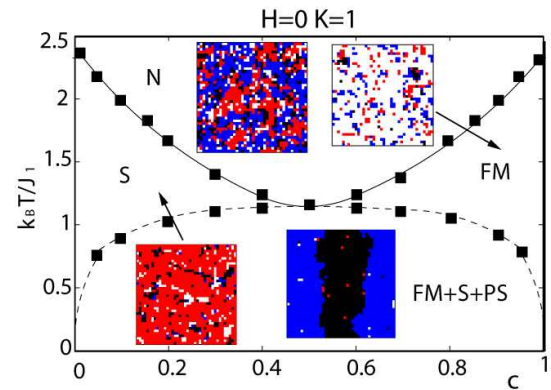


FIG. 1: (color online) Phase diagram, temperature (in units of  $J_1 = k_B$ ) versus concentration, in the absence of a magnetic field. N indicates the normal phase, S superconductivity, FM ferromagnetism, and PS phase separation. Solid lines represent second order phase transitions, dashed lines first order. Lines are guides to the eye. Snapshots of the simulation are shown. Black (white) represents  $s_i = 1$  ( $-1$ ), red (blue)  $s_i = 1$  ( $-1$ ).

Second, we consider the case  $K = 0.1$ . The results of the simulations are plotted in Fig. 2. We can understand the results as follows:  $J_2$  is much smaller than  $J_1$ , hence the spins will not pay much attention to the angular phases, and the part of the phase diagram concerning the spins will be very similar to the BEG model. Because  $J_2$  is so small, the phases will only order at very low temperatures (at zero concentration, the temperature is ten times lower than the one at which the spins order at a concentration of one). If the concentration is slightly raised from zero, the system is already in the phase separated regime. All the states with a nonzero phase have clustered, and are not diluted by states with nonzero spin. Therefore, the critical temperature in the phase separated region will approximately remain constant. Because the temperature at which the angular

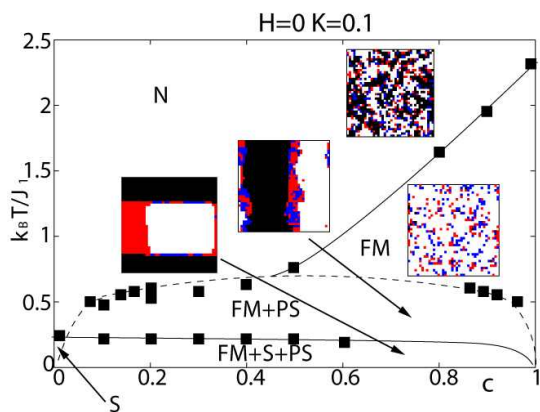


FIG. 2: (color online) Phase diagram in the absence of a magnetic field, for a relative coupling constant of  $K = 0.1$ .

phases order is lower than the temperature at which phase separation begins, there is a phase separated region in which the angular phases of the wavefunction are not ordered, which may appear unexpected at first sight. The transition within the phase separated region, from the region where the angular phases are not ordered to the phase where they are ordered (superconductivity), is second-order. This is expected, because in the phase separated region, all the phases have clustered, and the transition will be comparable with the transition in the Ising model, which is also second-order.

### C. Adding a magnetic field: the antiferromagnetic case

If we apply a nonnegative uniform magnetic field to the system, the ferro-antiferromagnetic symmetry is broken. We choose to consider the antiferromagnetic case here, because then there are two competing effects, the magnetic field tends to align the spins, whereas the exchange interaction wants to order the spins antiferromagnetically. The magnetic field  $H$  will be measured in units of  $J_1$ .

Kinle et al.<sup>5</sup> have studied the antiferromagnetic BEG model in the presence of a magnetic field, using Monte Carlo simulations. Their results at zero temperature suggest that the behavior of the system should be separated into three qualitatively distinct regions, namely  $H \in [0; 2]$ ;  $H \in [2; 4]$  and  $H \in [4; 1]$ . We consider here the cases  $K = 1$  and  $K = 0.1$  for values of  $H$  within each of these intervals.

#### 1. $H = 1.5$

First, we considered a magnetic field in the interval  $[0; 2]$ , namely  $H = 1.5$ . Both for  $K = 1$  and  $K = 0.1$ , the results (not shown) are qualitatively the same as in

the case of  $H = 0$ . This behavior was expected from the phase diagram of the single-component BEG model at zero temperature. Because the magnetic field tries to align the spins, the antiferromagnetic transition temperature is lower than in the absence of a magnetic field.

#### 2. $H = 2.5$

In the usual BEG model, the first-order phase transition disappears in the presence of a magnetic field  $H \in [2; 4]$ . At zero temperature, there is a second-order phase transition between a state with  $\langle s_i \rangle = 0$  at every site, and a checkerboard phase, where one sublattice has  $\langle s_i \rangle = 0$  at every site, and the other one  $\langle s_i \rangle = 1$ . There is also a transition between the checkerboard state, and an antiferromagnetic phase, but this transition is absent at nonzero temperature.<sup>5</sup>

For  $K = 1$ , the behavior of the two-component BEG model is still very similar to the case  $H = 0$ . For  $K = 0.1$ , the first-order phase transition disappears, and therefore there is no phase-separated region, see Fig. 3. We do observe an antiferromagnetic and a superconducting phase, but it is not clear from the figure whether the two phases overlap. To better understand this low- $T$  intermediate region, we also simulated the problem at a relative coupling strength of  $K = 0.5$ . In Fig. 4, we clearly observe that there is a region where antiferromagnetism and superconductivity coexist, without true phase separation, since the first-order phase transition has disappeared. What is also interesting is that at zero temperature this region begins at a nonzero concentration, and ends at a concentration smaller than one. When there is phase separation, this coexistence region always begins at  $c = 0$  and ends at  $c = 1$ .

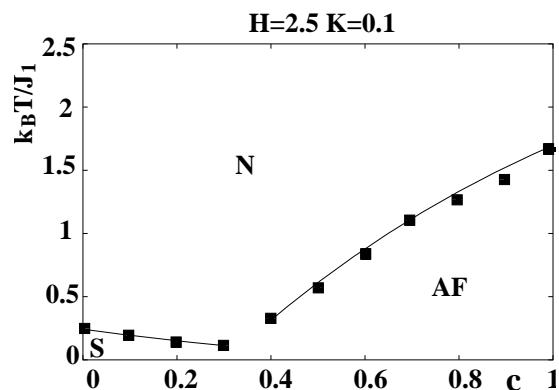


FIG. 3: Phase diagram at a magnetic field  $H = 2.5$  and relative exchange strength  $K = 0.1$ . N denotes the normal phase, S superconductivity and AF antiferromagnetism.

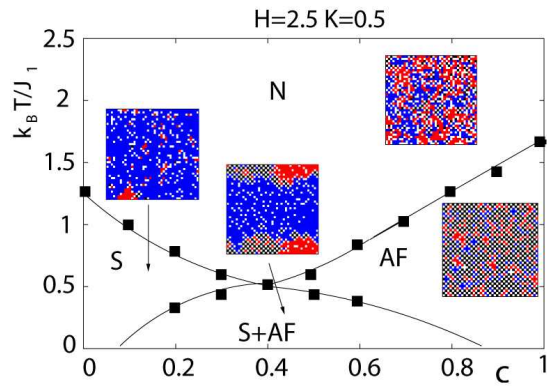


FIG. 4: (color online) Phase diagram at a magnetic field  $H = 2.5$  and relative exchange strength  $K = 0.5$ . There is a region where superconductivity and antiferromagnetism coexist, but where there is no true phase separation.

### 3. $H = 5$

In the original BEG model, when the magnetic field is increased to a value higher than  $H = 4$  at zero temperature, antiferromagnetism totally disappears because the spins tend to align with the magnetic field<sup>5</sup>. The system is therefore magnetized, but not because of the nearest-neighbor interactions. Therefore, this is not really ferromagnetism, but for the sake of simplicity, we denote it like this. For the case of  $K = 1$ , we observe a phase with ferromagnetic and superconducting ordering, and a ferromagnetic phase (not shown). For  $K = 0.1$ , we find another interesting phase, namely a ferromagnetic checkerboard phase, consisting of two sublattices, see Fig. 5. At the first sublattice, all sites are randomly occupied by phases with a value of  $s_i = 1$  or  $s_i = -1$ . At the second one, all sites are occupied by the spin that is favored by the magnetic field,  $s_i = 1$ . This phase is most likely to occur at a concentration of  $c = 0.5$  because in this case a perfect checkerboard is possible.

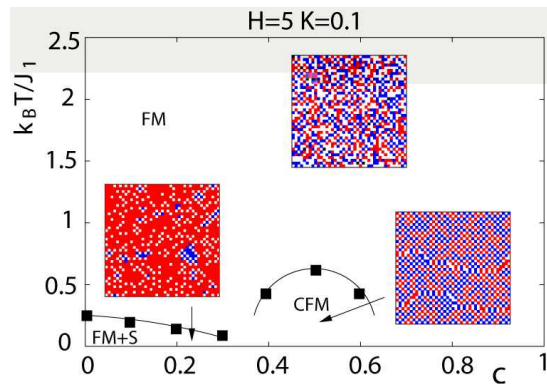


FIG. 5: (color online) Phase diagram at  $H = 5$  and  $K = 0.1$ . FM denotes ferromagnetism, S superconductivity and CFM denotes checkerboard ferromagnetism.

## III. ADDING A TRAP POTENTIAL

### A. The Blume-Emery-Griffiths model

Because experiments with cold atoms are often carried out in a trap, we will add a harmonic potential to the original BEG Hamiltonian, to describe mixtures of fermions and bosons in a trap. In general, the potential felt by the bosons is different from the one felt by the fermions, what implies that we must include two terms,

$$a_b \sum_i (x_i^2 + y_i^2) + a_f \sum_i (x_i^2 + y_i^2) (1 - s_i^2): \quad (7)$$

Here,  $x_i$  and  $y_i$  are the horizontal and vertical distances of site  $i$ , measured from the center of the lattice, in lattice units, and  $a_b$  and  $a_f$  measure how much the bosons (the states with  $s_i = 1$ ), and the fermions (the states with  $s_i = 0$ ) feel the influence of the trap. If  $a_b = a_f$ , this term is constant, and the phase diagram is not modified. We will consider the case  $a_b > a_f$ , which is the most relevant experimentally. Using the hard core constraint  $s_i^2 + s_i^2 = 1$ , we can then rewrite this term and add it to the BEG Hamiltonian, thus obtaining

$$H = J \sum_{\langle ij \rangle} s_i s_j + D \sum_i s_i^2 + a \sum_i (x_i^2 + y_i^2) s_i^2; \quad (8)$$

where  $a = a_b - a_f$ . This means that, effectively, the bosons will feel a stronger tendency to go to the center of the trap.

In the limit of  $a \ll 1$ , all the states with  $s_i = 1$  will cluster in the center of the trap, and therefore the ordering temperature will be the same as in the Ising model. Note that the maximum value of the extra term in the Hamiltonian will depend on the size of the lattice. This way of including the trapping potential is comparable with the work of Gygi et al.,<sup>6</sup> where a spatial-dependent chemical potential was added to the Bose-Hubbard model in order to describe bosonic atoms in an optical lattice.

We simulated the new model using the same procedures as for the BEG model and the two-component BEG model. The results for three different strengths of the trapping potential are plotted in Fig. 6. In the BEG model without a trap, there is a second-order phase transition from a normal state to an ordered state, and a first-order phase transition to a phase-separated region<sup>7</sup>. For the three values of  $a$  considered here, we do not find a first-order phase transition any more. A part of the first-order phase transition line disappears, and a part changes into a second-order one.

We see that for a small difference between the trap potential felt by the bosons and the fermions,  $a = J = 0.001$ , the transition temperatures are very similar to the case without a trap. For a large difference,  $a = J = 0.1$ , the transition temperatures approach the transition temperature of the Ising model for almost all concentrations, as expected. When the states with  $s_i = 1$  are ordered, we

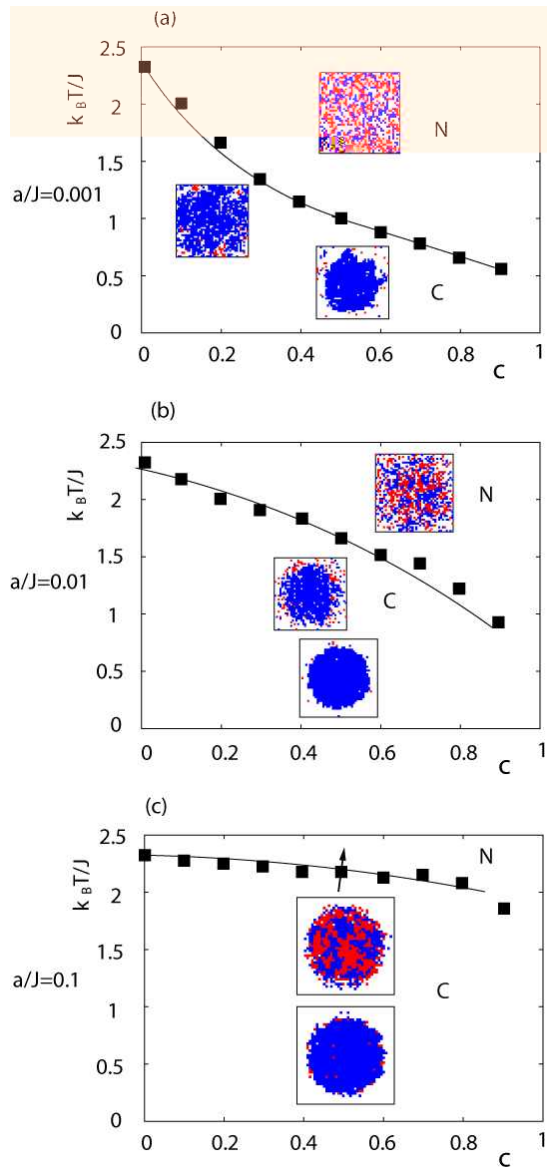


FIG. 6: (color online) Phase diagrams of the BEG model with a trapping potential. N denotes the normal, unordered state, C the condensed phase, in which the sites with  $s_i = 1$  are ordered. Lines are guides to the eyes. Snapshots are shown, where blue represents  $s_i = 1$ , red  $s_i = -1$ , and white  $s_i = 0$ .

will not speak of a superfluid state, but of a condensed state, because we now consider bosons in general.

It is important to estimate at which temperature the system starts to feel the influence of the trapping potential. Let us assume that a cluster of size  $m$  feels the potential when the energy difference between the state with this cluster in the center and in the corner of the lattice is of the order  $k_B T = J$ . For a lattice of size  $L^2$ , this estimation results in

$$\frac{m a L^2}{2J} \frac{k_B T}{J} : \quad (9)$$

In this approximation, a single particle ( $m = 1$ ) in a

lattice of size  $L = 41$  will start to feel the potential if  $k_B T = J = 800a$ . For  $a/J = 0.1$  and  $a/J = 0.01$  this results in  $k_B T = J = 80$  and  $k_B T = J = 8$ , respectively, in both cases much higher than the temperatures we are interested in, because ordering starts around  $k_B T = J = 2.4$ . Therefore, the single particles will experience the influence of the trap in the entire temperature range of Fig. 6 (b) and (c). For  $a/J = 0.001$ , a single particle will feel the trapping potential for temperatures lower than  $k_B T = J = 0.8$ . However, for higher temperatures the system already orders, and therefore there are some large clusters that according to Eq. (9) will feel the potential already at much higher temperatures. This reasoning is in agreement with the snapshots in Fig. 6 (a). For  $a/J = 0.001$ , we clearly observe the influence of the trap when the states with  $s_i = 1$  have clustered. In the disordered state, the influence is less visible. For  $a/J = 0.1$  and  $a/J = 0.01$ , we indeed see the influence of the trap for all temperatures, even in the disordered state.

### B. The two-component Bose-Einstein-Griffiths model

Analogous to the previous subsection, we will also add a trapping potential to the two-component BEG model. In the latter, both the states with  $s_i = 1$  and  $s_i = -1$  describe bosons, that both can condense. Therefore, this model can be applied to study cold atom mixtures with two species of bosons. We will consider the realistic case that the two species feel different trapping potentials. Therefore, we add the extra terms

$$a \sum_i (x_i^2 + y_i^2) s_i^2 + a_s \sum_i (x_i^2 + y_i^2) s_i^2 \quad (10)$$

to the Hamiltonian. Because at every lattice site  $s_i^2 + s_i^2 = 1$ , we can rewrite this term and add it to the two-component BEG Hamiltonian, to get

$$H = \sum_{ij} J_1 x_{ij} x_{ij} + \sum_{ij} J_2 s_{ij} s_{ij} + D \sum_i x_i^2 + a \sum_i (x_i^2 + y_i^2) s_i^2; \quad (11)$$

where  $a = a - a_s$  is now the difference between the potentials felt by the two species of bosons. Now, the bosons with  $s_i = 1$  have a stronger tendency to go to the center of the lattice.

The results of our simulations are plotted in Figs. 7 and 8. We considered two different strengths of the trapping potential, and two different ratios of the coupling strengths of the bosons, namely  $K = J_2 = J_1 = 1$  and  $K = 0.1$ . For  $K = 0.1$ , the right part of the first-order phase transition disappears and the left one becomes second-order (see Fig. 7), whereas for  $K = 1$  both left and right parts of the first-order phase transition are converted into second-order (see Fig. 8).

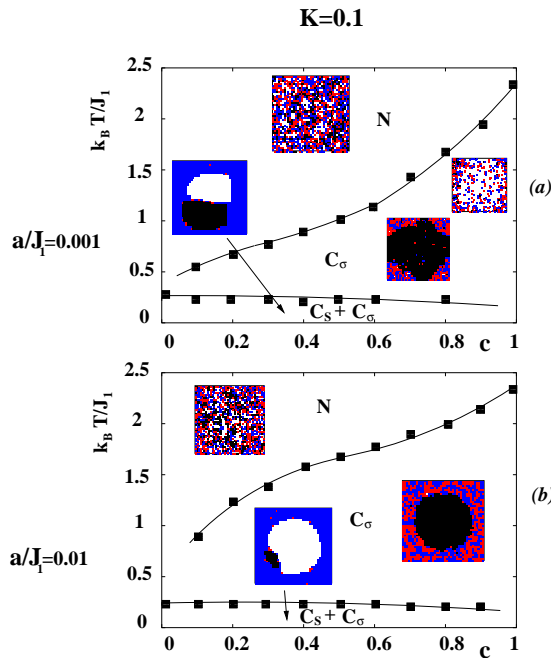


FIG. 7: (color online) Phase diagrams of the two-component BEG model with a trapping potential. N denotes the normal, unordered state,  $C_s$  and  $C_s$  the phases where the bosons represented by the state with  $s_i = 1$ , respectively  $s_i = -1$  are condensed. Lines are guides to the eyes. Snapshots are shown, where black and white represent  $s_i = 1$ , and red and blue  $s_i = -1$ .

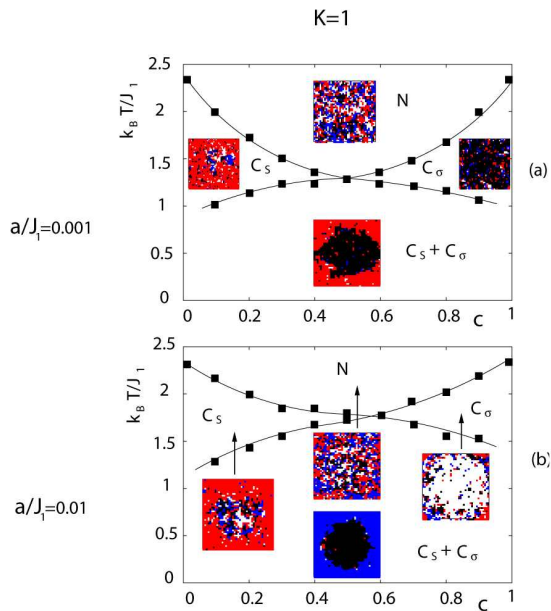


FIG. 8: (color online) Phase diagrams of the two-component BEG model with a trapping potential. The notation used is the same as in Fig. 7.

In the limit of  $a \ll 1$ , all the sites with  $s_i = 1$  will have clustered in the center of the lattice, and all sites

with  $s_i = -1$  at the corners. Therefore, for all concentrations, the system behaves as two uncoupled Ising models. In the case of  $K = 1$ , we see indeed that the transition temperatures for both species approach the Ising transition temperature. For  $K = 0.1$ , because  $J_2$  is ten times smaller than  $J_1$ , one of the species will order at the Ising transition temperature, and the other one at one tenth of the Ising transition temperature.

To find the temperature at which the system starts to feel the presence of the trap, we can make the same analysis as in subsection III A. Also here, we see in the snapshots of Figs. 7 and 8 that for  $a=J_1 = 0.1$  (not shown) and  $a=J_1 = 0.01$ , the system always feels the influence of the trap, and for  $a=J_1 = 0.001$ , it does only when the system is ordered. If we inspect Fig. 8 (a), we see that there is a phase  $C_s$  in which the bosons represented by  $s_i = 1$  are ordered, but the bosons represented by  $s_i = -1$  are not. This is somewhat surprising. A reason for the occurrence of this phase is that when all the bosons that have the tendency to go to the center of the trap have clustered there, automatically also the other bosons have clustered at the edge. Therefore, they can have nearest-neighbor interactions, and they can easily order. It remains to see whether such a phase indeed occurs in experiments. From the theoretical point of view, it would be interesting to also allow for states with  $s_i = s_i = 0$ , to verify the stability of this phase, when we relax the constraint that every lattice site must be occupied by one of the bosons. Note that for small enough concentrations, this phase will always occur, since the bosons are hardly diluted by the bosons.

#### IV. COMPARISON WITH EXPERIMENTS

##### A. Magnetic superconductors

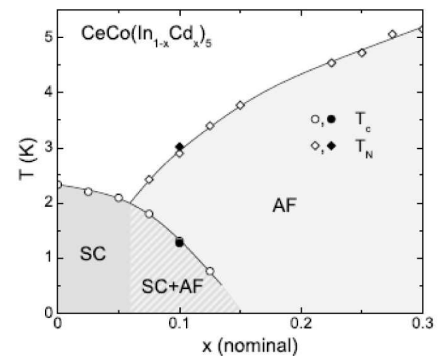


FIG. 9: Phase diagram of  $\text{CeCo}(\text{In}_{1-x}\text{Cd}_x)_5$ . The figure is extracted from Ref. 8.

There are several examples of Cerium-based superconductors, for example  $\text{CeCoIn}_5$  and  $\text{CeIrIn}_5$ , as well as antiferromagnets that contain this element, like  $\text{CeRhIn}_5$ ,

$\text{CeCoCd}_5$ ,  $\text{CeRhCd}_5$ , and  $\text{CeIrCd}_5$ . Let us consider  $\text{CeCoIn}_5$  and  $\text{CeCoCd}_5$ . These two materials have two elements in common, Ce and Co, and differ in the third element. By doping  $\text{CeCoIn}_5$  with Cd on the In site, we can change the superconductor  $\text{CeCoIn}_5$  into an antiferromagnet. There are more of these Cerium-based pairs, and therefore, this class of materials is appropriate for studying the interplay between superconductivity and magnetism.

Let us consider the heavy fermion superconductor  $\text{CeCoIn}_5$ , with Cadmium doping on the In-site. This material has the highest superconducting transition temperature ( $T_c = 2.3\text{K}$ ) of all heavy fermions, and its electronic structure is quasi-2D.<sup>7</sup> Nicklas et al.<sup>8</sup> and Pham et al.<sup>9</sup> determined the antiferromagnetic and superconducting onset temperatures of this material as a function of doping by elastic neutron scattering, specific heat, and resistivity measurements. Their results are plotted in Fig. 9. For experimental details we refer the reader to Ref. 8. The phase diagram of  $\text{CeCo}(\text{In}_{1-x}\text{Cd}_x)_5$  shows three ordered phases: a superconducting phase, a commensurate antiferromagnetic phase, and a region where superconductivity and antiferromagnetism microscopically coexist.

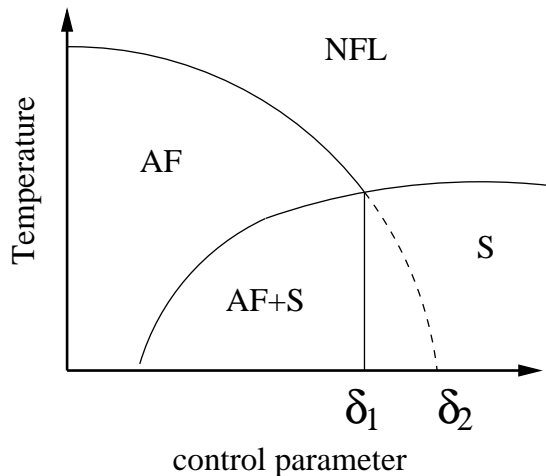


FIG. 10: Schematic phase diagram of unconventional superconductors in temperature-control parameter space. AF denotes antiferromagnetism, S superconductivity and NFL a non-Fermi liquid. Experimentally, antiferromagnetism often disappears abruptly at some critical value  $\delta_1$  of the control parameter, although one would expect a magnetic quantum critical point at some value  $\delta_2$  of the control parameter.

It is interesting to observe that in this material antiferromagnetism suddenly disappears at the point where the onset temperatures for superconductivity and antiferromagnetism are equal. This feature, however, may change in the presence of an applied magnetic field. In Fig. 10 we see a schematic phase diagram of unconventional superconductors, in temperature-control parameter space. In the case of  $\text{CeCo}(\text{In}_{1-x}\text{Cd}_x)_5$ , the control parameter would be doping. Another example of such a parameter

is pressure. Park et al.<sup>10</sup> determined the phase diagram of  $\text{CeRhIn}_5$  in temperature-pressure space with and without a magnetic field. Without a magnetic field, they also found this abrupt disappearance of the incommensurate antiferromagnetic order at  $\delta_1$ . However, when they applied a field of 33 kOe, the line of the magnetic ordering temperature went smoothly down to zero at  $\delta_2$ . Such a phase diagram shows many similarities with Fig. 4 if we identify pressure with inverse concentration in our model. Indeed, for an external magnetic field of  $H = 2.5$  and a relative exchange strength  $K = 0.5$  (see Fig. 4), the phase diagram shows the same three ordered phases. Further, the coexisting phase is not phase separated.

Finally, we consider the compound  $\text{CeIr}(\text{In}_{1-x}\text{Cd}_x)_5$ , see Fig. 11 and Ref. 9. For this material, it is not clear if there is a region where superconductivity and magnetism coexist. If there is such a region, it is in a small doping interval. The phase diagram of this material strongly resembles the phase diagram of the two-component BEG model with an external magnetic field of  $H = 2.5$  and a relative coupling strength of  $K = 0.1$ , see Fig. 3. Although this experiment was also carried out without an external magnetic field, we only find similarities with our model in the presence of a magnetic field.

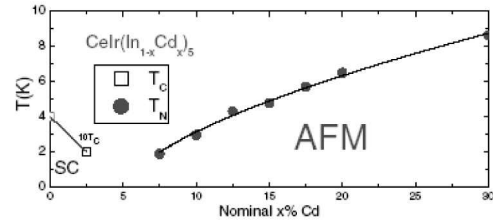


FIG. 11: Phase diagram of the heavy fermion  $\text{CeIr}(\text{In}_{1-x}\text{Cd}_x)_5$ . The figure is extracted from Ref. 9.

## B. Cold atom systems

In 2006, two experimental groups, the group of Ketterle at MIT,<sup>11</sup> and the group of Hulet at Rice University,<sup>12</sup> have performed experiments with imbalanced ultracold  $^6\text{Li}$  atoms in a trap, and obtained contradictory results. The MIT group measured a transition between a normal and a superfluid phase at a polarization of  $P = 0.70$ , whereas the group at Rice University observed a transition between two superfluid phases at  $P = 0.09$ . Here,  $P$  measures the imbalance between the spin-up and the spin-down atoms,

$$P = \frac{N_{\uparrow} - N_{\downarrow}}{N_{\uparrow} + N_{\downarrow}} \quad (12)$$

Gubbels et al.<sup>13</sup> have set up a theoretical model to describe these imbalanced Fermi mixtures and determined a general phase diagram in temperature-polarization space that can explain the observations of both groups. The

topology of their phase diagram shows large similarities with the phase diagram of the BEG model. We can understand this resemblance as follows. In the BEG model, the concentration  $c$  is the fraction of lattice sites with  $n_i = 0$ , and thus the fraction of the system that cannot condense. The polarization  $P$  is a measure for the difference of the atoms in the spin-up and the spin-down state, and thus for the number of fermions that remain after the others have paired. The atoms with spin up and spin down will form pairs, and such a pair can be described as a boson. Therefore, the polarization is also a measure for the fraction of the system that cannot condense, and the concentration can be mapped onto the polarization. We can identify the paired atoms, the preformed bosons, with the states  $n_i = 1$ , and the remaining fermions with  $n_i = 0$ , see Fig. 12.

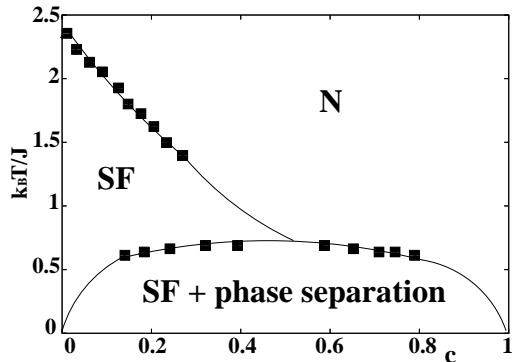


FIG. 12: Phase diagram of the original BEG model, obtained by Monte Carlo simulations. N denotes the normal phase, SF superfluidity. Lines are guides to the eyes. The transition between the normal and the superfluid state is second-order, the transition to the phase separated regime is first-order.

The experiments with  $^6\text{Li}$  are carried out in a trap, and the theoretical model of Gubbels et al. only includes the presence of the trap by using the local density approximation. Now, we would like to compare their phase diagram with our results of the BEG model with a trapping potential, in Figs. 7 and 8. Although in the case of imbalanced fermions the frequency  $\omega$  of the optical trap felt by the pairs of fermions (bosons) and the remaining unpaired fermions is the same, the mass of the bosons is twice as large, and the potential constant  $a_b$  is thus larger than  $a_f$ . This means that the comparison must be made with the BEG model in a trap. In this model, the first-order phase transition, measured by a jump in the concentration as a function of the anisotropy field  $D$  has disappeared, thus there is no true transition to a phase-separated regime. However, if we inspect the snapshots, we see that for low enough temperatures, or large enough trapping potential, there still is a clear separation between the condensed bosons and the fermions, suggesting some kind of effective phase separation. We

note that in experiments, phase separation is measured by inspecting the radii of the clouds of the atoms in the different hyperfine states, and not by a jump in some order parameter.<sup>12</sup> Our results thus suggest that the measured different radii are not per se an evidence of a true thermodynamic phase separation. Further experiments are required to clarify this issue.

Although our model describes qualitatively the experimentally observed phases, it cannot capture the fine details of recent experimental results. Studies by Shin et al.<sup>14</sup> indicate that there is no superfluid phase, or phase-separated phase for polarizations above  $P = 0.36$ . By a quantum Monte Carlo approach, Lobo et al.<sup>15</sup> predict a phase transition between a normal and a superfluid state at a polarization of  $P = 0.39$  at zero temperature, and Gubbels and Stoof<sup>6</sup> recovered this result using a Wilsonian renormalization group theory.

## V. CONCLUSIONS

We simulated a two-component extension of the BEG model without an external magnetic field and determined the phase diagram in the concentration-temperature space. In the region where magnetism and superconductivity coexist, the system is always phase separated. We added a magnetic field to our model, and considered the antiferromagnetic case. In this case, we also find phase diagrams with true coexistence of two ordered phases. These diagrams are comparable with the phase diagram of doped heavy fermions in the presence of a magnetic field.

In order to describe cold atom systems, we added a trapping potential to the BEG model, and our extension of this model. The added potential changes the phase separation regime conceptually. We cannot speak anymore about true phase separation, but more about a crossover to a phase separated region. We argue that the BEG model with a trapping potential can be used to model imbalanced Fermi mixtures. However, there are still quantitative differences with experiments, which our model is not able to cover. We also made predictions for the phase diagram of boson-boson mixtures based on our simulations of the two-component BEG model with a trapping potential. Although there is no available experimental data on boson-boson mixtures, we hope that our work can motivate further studies in this direction.

## VI. ACKNOWLEDGEMENTS

We are grateful to K. Gubbels, H. van Beijeren, A. de Vries and R. Movshovich for fruitful discussions and to J. de Graaf for technical help.

- 
- <sup>1</sup> E.H. Graf, D.M. Lee, and John D. Reppy, *Phys. Rev. Lett.* 19, 417 (1967).
  - <sup>2</sup> M. Blume, V.J. Emery and R.B. Griffiths, *Phys. Rev. A* 4, 1071 (1971).
  - <sup>3</sup> A. Falicov and A. Berker, *Phys. Rev. Lett.* 74, 426 (1995).
  - <sup>4</sup> M. Chan, N. Mulders and J. Reppy, *Physics Today* 49, 30 (1996).
  - <sup>5</sup> J.D. Kinell, Per Amund Rikvold and Yung-Li Wang, *Phys. Rev. B* 45, 7237 (1992).
  - <sup>6</sup> Olivier Gyi, Helmut G. Katzgraber, Matthias Troyer, Stefan Wessel and G. George Batrouni, *Phys. Rev. A* 73, 063606 (2006).
  - <sup>7</sup> H. Shishido et al., *J. Phys. Soc. Jpn* 71, 162 (2002).
  - <sup>8</sup> M. Nicklas, O. Stockert, Tuson Park, K. Habicht, K. Kiefer, L.D. Pham, J.D. Thompson, Z. Fisk, and F. Steglich, *Phys. Rev. B* 76, 052401 (2007).
  - <sup>9</sup> L.D. Pham, Tuson Park, S.M. Aquilino, J.D. Thompson, and Z. Fisk, *Phys. Rev. Lett.* 97, 056404 (2006).
  - <sup>10</sup> Tuson Park, F. Ronning, H.Q. Yuan, M.B. Salamon, R. Movshovich, J.L. Sarrao, J.D. Thompson, *Nature* 440, 65 (2006).
  - <sup>11</sup> Martin W. Zwierlein, Christian H. Schunck, Andre Schirotzek, Wolfgang Ketterle, *Nature* 442, 54 (2006).
  - <sup>12</sup> Guthrie B. Partridge, Wenhui Li, Ramsey I. Kamar, Yean-an Liao, and Randall G. Hulet, *Science* 311, 503 (2006).
  - <sup>13</sup> K.B. Gubbels, M.W.J. Romans, and H.T.C. Stoof, *Phys. Rev. Lett.* 97, 210402 (2006).
  - <sup>14</sup> Yong-il Shin, Christian H. Schunck, Andre Schirotzek, Wolfgang Ketterle, *Nature* 451, 689 (2008).
  - <sup>15</sup> C. Lobo, A. Recati, S. Giorgini, and S. Stringari, *Phys. Rev. Lett.* 97, 200403 (2006).
  - <sup>16</sup> K.B. Gubbels and H.T.C. Stoof, *Phys. Rev. Lett.* 100, 140407 (2008).